

ICM11

Influence of austenite stability on predicted cyclic stress-strain response of metastable austenitic steels

G.R. Lehnhoff^{a*} and K.O. Findley^a

^a*Department of Metallurgical and Materials Engineering, Colorado School of Mines, Golden, CO 80401 USA*

Abstract

A modeling approach that captures the plastic strain amplitude dependence of strain induced martensite fraction evolution during low cycle fatigue (LCF) loading of metastable austenitic steels has been developed. The model is based on a modified version of the Olson-Cohen kinetic equation that retains connection to the underlying mechanisms of the transformation by relating cyclic austenite stability to monotonic stability. The kinetic model is then input into an evolving composite mechanical model that relies on a simple rule of mixtures formulation to predict cyclic stress-strain behavior, including increases in stress amplitude due to martensitic transformation. Predictions from the modeling approach compare well to fatigue data in the literature for AISI 304 stainless steel.

© 2011 Published by Elsevier Ltd. Open access under [CC BY-NC-ND license](https://creativecommons.org/licenses/by-nc-nd/4.0/).

Selection and peer-review under responsibility of ICM11

Keywords: austenite stability; martensite; phase transformation; low cycle fatigue; cyclic hardening

1. Introduction

Metastable austenite can undergo progressive strain induced martensitic transformation (SIMT) during cyclic loading. In monotonic loading, the austenite stability has been linked to multiple factors including grain size, morphology, and composition [1–3]. Similar factors likely affect SIMT during fatigue cycling [4–6]. Furthermore, the extent of martensitic transformation is a function of both the cyclic strain amplitude and the amount of accumulated plastic strain during cyclic loading [6,7].

Strain induced martensite nucleation occurs on shear band intersections, which can be composed of mechanical twins, stacking fault bundles, or epsilon (hcp) martensite. To characterize the evolution of

* Corresponding author. Tel.: +1 303 273 3788; fax: +1 303 273 3016

E-mail address: glehnhof@mymail.mines.edu

martensite volume fraction (V_α) as a function of applied plastic strain (ε), Olson and Cohen developed the following model for the kinetics of SIMT during monotonic loading of fully austenitic steels (Eq. 1):

$$V_\alpha = 1 - \exp\{-\beta_m [1 - \exp(-\alpha_m \varepsilon)]^{n_m}\} \quad (1)$$

where subscript m indicates monotonic loading, α scales with the ease of shear band formation, β scales with the probability of a shear band intersection forming a martensite nucleus, and n relates the number of shear bands to the number of shear band intersections [8]. For the case of randomly oriented shear bands, n is 2, but n is anticipated to be smaller at low strains and larger at high strains due to activation of more slip systems at higher strains. Typically, n is chosen to reflect the latter case.

Similar approaches have been utilized to capture the martensite volume fraction evolution as a function of cumulative plastic strain (λ) during low cycle fatigue (LCF) loading, although the transformation kinetics have additionally been shown to depend on the applied plastic strain amplitude ($\varepsilon_{a,p}$). Smaga *et al.* accounted for this by introducing the concept of a cumulative strain energy density that scales with plastic strain amplitude [6]. While this model is successful in predicting the martensite volume fraction evolution, the model parameters are largely empirical and do not take into account the fundamental mechanisms of SIMT, unlike the monotonic Olson-Cohen model. Tomita and Iwamoto adapted the Olson-Cohen model (Eq. 1) to LCF loading by replacing monotonic plastic strain (ε) with cumulative plastic strain (λ) and using α_c , β_c , and n_c parameters as the fatigue corollaries to the monotonic parameters (indicated by a subscript c for cyclic loading) [9]. Again, this adapted model is more empirical than physically-based because the $\varepsilon_{a,p}$ dependence of the parameters is based solely on regression analysis.

The stress amplitude (σ_a) as a function of number of cycles for metastable austenitic steels during LCF depends on microstructure evolution and can be divided into three regimes. At low levels of cumulative plastic strain (initial cycles), little martensite is formed and the stress amplitude depends on austenite substructure development and cyclic hardening/softening of austenite; this is termed the cyclic incubation regime. At a critical level of cumulative plastic strain, the martensitic transformation proceeds readily, resulting in pronounced increases in σ_a ; this is termed the cyclic transformation regime. In some cases, the transformation may reach a cyclic saturation regime, in which limited transformation occurs with further cycling [7,10].

2. Modeling approach

Modeling in this study has been divided into two parts: modeling of cyclic SIMT kinetics and modeling of cyclic stress-strain response. In both cases, the modeling is based on experimental fatigue data of AISI 304 austenitic stainless steel tested at plastic strain amplitudes ranging from $\varepsilon_{a,p} = 0.2\%$ to $\varepsilon_{a,p} = 0.6\%$ obtained by Smaga *et al.* [6].

2.1. Cyclic SIMT Kinetic Model

The goal of modeling SIMT kinetics during cyclic loading is to establish the strain amplitude dependence of the cyclic kinetic parameters (α_c , β_c , and n_c) from a fundamental standpoint that considers monotonic loading as a limiting case. If the plastic strain amplitude is high enough, martensite formation will occur during the first 1/4 cycle with $\lambda = \varepsilon$ before the first load reversal. This specific case can be used to relate the cyclic kinetic parameters to the monotonic kinetic parameters, with differences between the two parameters sets and the plastic strain amplitude dependence during cyclic loading being based on the underlying fundamentals of SIMT. For this purpose, if a subscript m or c is not specified, the discussion applies to both monotonic and cyclic loading.

The kinetic parameter n relates the number of shear bands to shear band intersections, and thus depends on the number of active slip systems. During monotonic loading, multiple slip is likely to occur

and thus n_m is expected to be high. However, during LCF, the nominal plastic strains are small, and fewer slip systems are expected to be activated, suggesting n_c is less than n_m . Also, it is expected that the number of activated secondary slip systems increases with plastic strain amplitude, as suggested by LCF modeling of the austenite phase in a duplex stainless steel [11]. Therefore, n_c is expected to increase with plastic strain amplitude. The n parameter can be estimated as the slope of a plot of $\ln(\ln(1-V_a)^{-1})$ vs. $\ln(\varepsilon)$ for monotonic loading or, by analogy, vs. $\ln(\lambda)$ for cyclic loading [3]. Based on the data presented by Smaga *et al.*, it was determined that n_m is 4.0 and on average n_c is 2.2 for the 304SS at all applied plastic strain amplitudes. For the other two metastable austenitic stainless steels considered in the study (AISI 321 and AISI 348), an n_c value of 2.2 is also reasonable [6]. Thus, n_c is less than n_m as expected, but n_c does not increase with increases in plastic strain amplitude. Nonetheless, it is hypothesized that if additional tests were run at larger values of $\varepsilon_{a,p}$, n_c may increase.

The β parameter relates to the probability of a shear band intersection forming a martensite nucleus and should be dictated by thermodynamics of the austenite to martensite transformation. Because the thermodynamics are largely unaffected by whether one considers monotonic plastic strain or cumulative plastic strain, it is expected that the β parameter is constant across all monotonic and cyclic cases. Accordingly, a value of $\beta_c = \beta_m = 3.34$ obtained through regression analysis of the monotonic data was used in all cases.

Finally, the α parameter relates to the ease of shear band formation with applied monotonic or cumulative plastic strain. It is experimentally observed that the critical cumulative plastic strain where SIMT is observed is much larger than the critical monotonic plastic strain. This implies that fatigue loading is inherently less efficient at generating shear bands than monotonic loading and that α_c should be less than α_m . It is further expected that α_c should increase as $\varepsilon_{a,p}$ increases based on the modeling results of Evrard *et al.* who showed slip system activity increases with increasing applied strain amplitude in the austenite phase of a duplex stainless steel [11]. This modeling result is in agreement with the concept of a plastic strain amplitude-dependent cumulative strain energy density introduced by Smaga *et al.* [6]. To capture this behavior the following formulation for α_c is proposed:

$$\alpha_c = [(\varepsilon_{a,p} - \varepsilon_{a,p,*}) / (\varepsilon_{m,*} - \varepsilon_{a,p,*})]^r \alpha_m \quad (2)$$

where $\varepsilon_{a,p,*}$ is the critical plastic strain amplitude below which minimal martensite is formed even at high cumulative plastic strains, $\varepsilon_{m,*}$ is the critical monotonic plastic strain below which minimal martensite is formed, and r is constant for a given material. These critical terms define the range of plastic strain amplitudes under which cumulative SIMT operates: below $\varepsilon_{a,p,*}$ there is no significant transformation, while above $\varepsilon_{m,*}$ transformation will be induced due to monotonic loading in the first 1/4 cycle before load reversal. The bracketed term therefore signifies the fraction of the possible plastic strain amplitude range for LCF SIMT a given $\varepsilon_{a,p}$ represents and allows α_c to vary from 0 to α_m over this range. The r exponent simply accounts for the fact that the plastic strain amplitude dependence of α_c is not necessarily linear. $\varepsilon_{m,*}$ is 20% (Fig. 1), $\varepsilon_{a,p,*}$ is 0.2% (Fig. 2c), α_m is 0.865, and r is 1.18, the latter two determined from regression analysis, for the AISI 304 experimental fatigue data.

2.2. Cyclic Stress-Strain Mechanical Model

A model has been developed to correlate martensitic transformation with the cyclic stress-strain response of metastable austenitic steel, specifically by capturing the dramatic increases in stress amplitude observed during the cyclic transformation regime in strain-controlled fatigue experiments. The model calculates the elastic and plastic segments of the stress-strain curve for the tension and compression portions of each cycle with the volume fraction of martensite being updated continuously with cumulative plastic strain. The elastic region is determined by a simple rule of mixtures approximation of the yield strength (Eq. 3) by using single phase austenite and martensite mechanical

properties, while the plastic region uses a flow stress rule of mixtures that is modified for LCF loading (Eq. 4).

$$\Delta\sigma_{ys} = 2\{[1 - V_{\alpha'}]\sigma_{ys}^{\gamma} + V_{\alpha'}\sigma_{ys}^{\alpha'}\} \quad (3)$$

$$\Delta\sigma_{flow} = 2\{[1 - V_{\alpha'}][\sigma_{flow}^{\gamma}(\Delta\varepsilon/2)] + V_{\alpha'}[\sigma_{flow}^{\alpha'}(\Delta\varepsilon/2)]\} \quad (4)$$

In Eqs. 3 and 4, y_s stands for yield strength, γ indicates behavior of single phase austenite, and α' indicates behavior of single phase martensite. Because it is difficult to determine the single phase properties of austenite and martensite due to the metastability of the austenite, stress-strain data for a stable austenitic stainless steel (AISI 316) and a martensitic stainless steel (AISI 410) were used to approximate the individual phase strengths in the rule of mixtures [12]. The model employs total strain control (in contrast to the case of plastic strain control considered up until now), and to a first approximation, assumes that the plastic strain amplitude is constant (equal to $\varepsilon_{a,p}$ for the first cycle) for a given total strain amplitude when calculating α_c for the kinetic model. In reality, the plastic strain amplitude decreases with increases in stress amplitude due to the martensitic transformation. One option is to correlate the models to experiments performed in plastic strain control. However, it is difficult to perform experiments using plastic strain control because a single modulus value must be used throughout the experiment to calculate plastic strain. The measured modulus may change during fatigue cycling due to changes in compliance or other factors, which would render the calculated plastic strain control inaccurate [13,14]. Thus, the models were developed assuming total strain control so they can be correlated to LCF experiments conducted without any assumptions about material behavior.

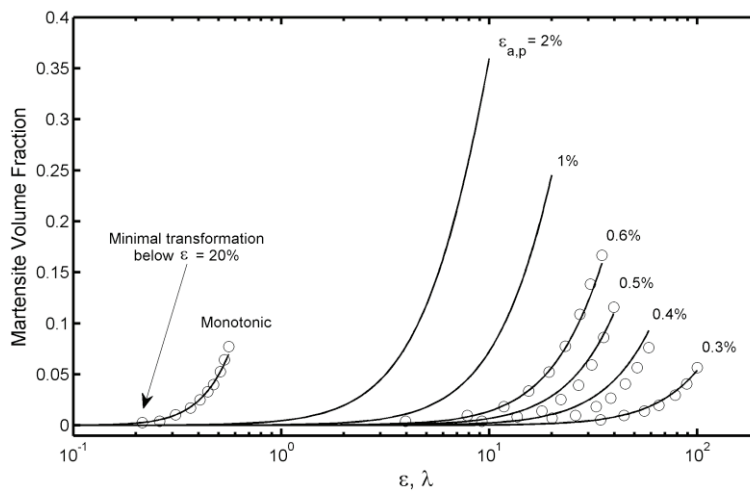


Fig. 1. Monotonic and cyclic SIMT kinetics as a function of plastic strain (ε) and cumulative plastic strain (λ), respectively at a variety of plastic strain amplitudes ($\varepsilon_{a,p}$). Open circles correspond to data adapted from Smaga *et al.* and lines correspond to model predictions [6]. The arrow at $\varepsilon = 20\%$ for monotonic loading signifies the critical monotonic plastic strain below which minimal martensite is formed, $\varepsilon_{m,*}$.

3. Results and discussion

Fig. 1 shows the monotonic and cyclic SIMT kinetic data for the AISI 304 austenitic stainless steel investigated by Smaga *et al.* as well as the transformation kinetics predicted by the Cyclic SIMT Kinetic Model [6]. The proposed model agrees reasonably well with the experimental data over a wide range of applied plastic strain amplitudes and cumulative plastic strains.

The influence of the austenite to martensite transformation on the LCF hysteresis loops calculated by the cyclic stress-strain model is shown in Fig. 2a for an applied total strain amplitude of 0.8% (initial plastic strain amplitude of roughly 0.65%). The hysteresis loops achieve higher stress levels with increasing cycle number due to martensite formation, accompanied by a slight decrease in plastic strain amplitude. The latter effect's continual influence on SIMT kinetics is not taken into account by the Cyclic Stress-Strain Mechanical Model but is a reasonable omission for a simple approximation. The predicted stress amplitude evolution as a function of cycle number (N) at several applied total strain amplitudes is shown in Fig. 2b and can be compared to the experimental results of Smaga *et al.* shown in Fig. 2c [6]. Again, reasonable agreement between the mechanical model and experimental results is achieved, although the experimental results are not precisely comparable due to the different strain control conditions. Because the mechanical model only accounts for cyclic hardening in terms of an increased martensite fraction, the reasonable correlation between the model predictions and experimental results confirms that the martensite fraction evolution, and therefore austenite stability, dominate the mechanical response in the cyclic transformation regime. This result highlights the importance of understanding austenite stability during cyclic loading.

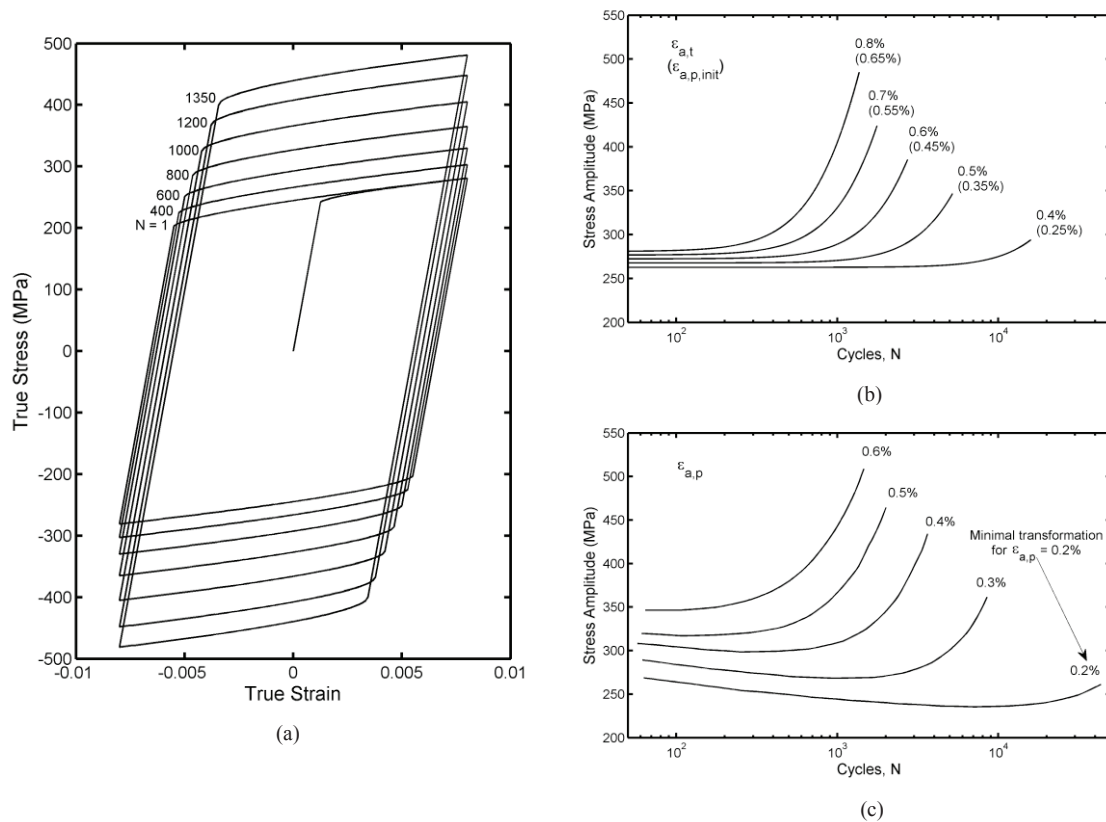


Fig. 2. (a) Predicted evolution of cyclic stress-strain curves for various cycles (N) at a total strain amplitude $\epsilon_{a,t} = 0.8\%$ (initial plastic strain amplitude $\epsilon_{a,p,init} \approx 0.65\%$). (b) Predicted evolution of stress amplitude (σ_a) with cycle number for various total strain amplitudes (and corresponding initial plastic strain amplitudes). (c) Evolution of stress amplitude observed by Smaga *et al.* under plastic strain control ($\epsilon_{a,p}$) [6]. Note that at $\epsilon_{a,p} = 0.2\%$ in (c), minimal hardening due to transformation is observed even at high cumulative plastic strains and thus is used to establish $\epsilon_{a,p}^* = 0.2\%$.

4. Conclusions

A model for cyclic SIMT kinetics that accounts for the strain amplitude dependence of the transformation and relates cyclic austenite stability to monotonic austenite stability is proposed. The kinetic model can then be input into an evolving composite mechanical model that predicts the influence of martensitic transformation on the cyclic stress-strain evolution of metastable austenitic steels. In both cases, the models offer reasonable agreement to experimental data of AISI 304 austenitic stainless steel [6]. The results highlight the importance of the martensitic transformation and austenite stability in dictating the LCF response of metastable austenite.

Acknowledgements

This material is based upon work supported by the National Science Foundation under Grant No. 0955236. This research was supported in part by an award from the Department of Energy (DOE) Office of Science Graduate Fellowship Program (DOE SCGF). The DOE SCGF Program was made possible in part by the American Recovery and Reinvestment Act of 2009. The DOE SCGF program is administered by the Oak Ridge Institute for Science and Education for the DOE. ORISE is managed by Oak Ridge Associated Universities (ORAU) under DOE contract number DE-AC05-06OR23100. All opinions expressed in this paper are the authors' and do not necessarily reflect the policies and views of DOE, ORAU, or ORISE. The authors also gratefully acknowledge the support of the Advanced Steel Processing and Products Research Center, a university-industry cooperative research center.

References

- [1] Basuki A, Aernoudt E. Influence of rolling of TRIP steel in the intercritical region on the stability of retained austenite. *J Mat Proc Tech* 1999;**89–90**:37–43.
- [2] Timokhina IB, Hodgson PD, Pereloma EV. Effect of microstructure on the stability of retained austenite in transformation-induced-plasticity steels. *Met & Mat Trans A* 2004;**35**:2331–41.
- [3] Samek L, De Moor E, Penning J, De Cooman BC. Influence of alloying elements on the kinetics of strain-induced martensite nucleation in low-alloy, multiphase high-strength steels. *Met & Mat Trans A* 2006;**37**:109–24.
- [4] Stolarz J, Baffie N, Magnin T. Fatigue short crack behavior in metastable austenitic stainless steels with different grain sizes. *Mat Sci & Eng A* 2001;**319–321**:521–6.
- [5] Basu K, Das M, Bhattacharjee D, Chakraborti PC. Effect of grain size on austenite stability and room temperature low cycle fatigue behaviour of solution annealed AISI 316LN austenitic stainless steel. *Mat Sci & Tech* 2007;**23**:1278–84.
- [6] Smaga M, Walther F, Eifler D. Deformation-induced martensitic transformation in metastable austenitic steels. *Mat Sci & Eng A* 2008;**483–484**:394–7.
- [7] Glage A, Weidner A, Biermann H. Effect of austenite stability on the low cycle fatigue behavior and microstructure of high alloyed metastable austenitic cast TRIP steels. *Procedia Eng* 2010;**2**:2085–94.
- [8] Olson GB, Cohen M. Kinetics of strain-induced martensitic nucleation. *Met Trans A* 1975;**6**:791–5.
- [9] Tomita Y, Iwamoto T. Computational prediction of deformation behavior of TRIP steels under cyclic loading. *Int J Mech Sci* 2001;**43**:2017–34.
- [10] Ye D, Matsuoka S, Nagashima N, Suzuki N. The low cycle fatigue, deformation, and final fracture behaviour of an austenitic stainless steel. *Mat Sci & Eng A* 2006;**415**:104–17.
- [11] Evrard P, Alvarez-Armas I, Aubin V, Degallaix S. Polycrystalline modeling of the cyclic hardening/softening behavior of an austenitic-ferritic stainless steel. *Mech of Mat* 2010;**42**:395–404.
- [12] *Atlas of stress-strain curves*. 2nd ed. Ohio: ASM International; 2002.
- [13] Ye D, Xu Y, Xiao L, Cha H. Effects of low-cycle fatigue on static mechanical properties, microstructures and fracture behavior of 304 stainless steel. *Mat Sci & Eng A* 2010;**527**:4092–4102.
- [14] Bayerlein M, Mughrabi H, Kesten M, Meier B. Improvement of the strength of a metastable austenitic stainless steel by cyclic deformation-induced martensitic transformation at 103 K. *Mat Sci & Eng A* 1992;**159**:35–41.